Article

Influence of a Polar Near-Neighbor on Incipient Proton Transfer in a Strongly Hydrogen Bonded Complex

Sherri W. Hunt, Kelly J. Higgins, Matthew B. Craddock, Carolyn S. Brauer, and Kenneth R. Leopold

J. Am. Chem. Soc., **2003**, 125 (45), 13850-13860• DOI: 10.1021/ja030435x • Publication Date (Web): 15 October 2003

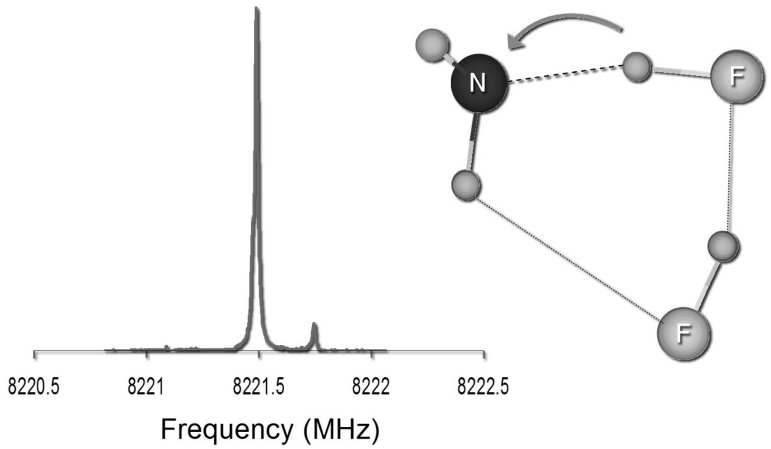

More About This Article

Additional resources and features associated with this article are available within the HTML version:

- Supporting Information
- Links to the 4 articles that cite this article, as of the time of this article download
- Access to high resolution figures
- Links to articles and content related to this article
- Copyright permission to reproduce figures and/or text from this article

View the Full Text HTML

J|A|C|S
ARTICLES
Published on Web 10/15/2003

Influence of a Polar Near-Neighbor on Incipient Proton Transfer in a Strongly Hydrogen Bonded Complex

Sherri W. Hunt,† Kelly J. Higgins,‡ Matthew B. Craddock, Carolyn S. Brauer, and Kenneth R. Leopold*

Contribution from the Department of Chemistry, University of Minnesota, 207 Pleasant Street, SE, Minneapolis, Minnesota 55455

Received July 17, 2003; E-mail: kleopold@chem.umn.edu

Abstract: Rotational spectroscopy and ab initio calculations have been used to characterize the complexes H_3N-HF and $H_3N-HF-HF$ in the gas phase. H_3N-HF is a C_{3v} symmetric, hydrogen bonded system with an NF distance of 2.640(21) Å and an N···H hydrogen bond length of 1.693(42) Å. The $H_3N-HF-HF$ complex, on the other hand, forms a six-membered HN−HF−HF ring, in which both the linear hydrogen bond in the H_3N-HF moiety and the F−H−F angle of $(HF)_2$ are perturbed relative to those in the corresponding dimers. The N···F and F···F distances in the trimer are 2.4509(74) Å and 2.651(11) Å, respectively. The N···H hydrogen bond length in $H_3N-HF-HF$ is 1.488(12) Å, a value which is 0.205(54) Å shorter than that in H_3N-HF. Similarly, the F···F distance, 2.651(11) Å, is 0.13(2) Å shorter than that in $(HF)_2$. Counterpoise-corrected geometry optimizations are presented, which are in good agreement with the experimental structures for both the dimer and trimer, and further characterize small, but significant, changes in the NH_3 and HF subunits upon complexation. Analysis of internal rotation in the spectrum of $H_3N-HF-HF$ gives the potential barrier for internal rotation of the NH_3 unit, V_3, to be 118(2) cm^{-1}. Ab initio calculations reproduce this number to within 10% if the monomer units and the molecular frame are allowed to fully relax as the internal rotation takes place. The binding energies of H_3N-HF and $H_3N-HF-HF$, calculated at the MP2/aug-cc-pVTZ level and corrected for basis set superposition error are 12.3 and 22.0 kcal/mol, respectively. Additional energy calculations have been performed to explore the lowest frequency vibration of $H_3N-HF-HF$, a ring-opening motion that increases the NFF angle. The addition of one HF molecule to H_3N-HF represents the first step of microsolvation of a hydrogen bonded complex and the results of this study demonstrate that a single, polar near-neighbor has a significant influence on the extent of proton transfer across the hydrogen bond. As measured using the proton-transfer parameter ρ_{PT}, previously defined by Kurnig and Scheiner [*Int. J. Quantum Chem., Quantum Biol. Symp.* **1987**, *14*, 47], the degree of proton transfer in $H_3N-HF-HF$ is greater than that in either $(CH_3)_3N-HF$ or H_3N-HCl but less than that in $(CH_3)_3N-HCl$.

Introduction

The importance of hydrogen bonding was recognized well over a half century ago,[1] and since that time, the study of its connection to proton-transfer processes has been an active area of investigation.[1c,2] Indeed, since the earliest quantum mechanical descriptions were formulated,[3] the study of hydrogen bonding and proton transfer has grown to encompass numerous topics including inter-[2,4] and intramolecular[5] proton-transfer dynamics, medium[6] and electric field[7] effects, excited-state proton transfer,[8] proton-coupled electron transfer,[9] and a class of so-called "very strong" hydrogen bonds.[10] Spectroscopic

† Present Address: Department of Chemistry, University of California, Irvine, CA 92697-2025.

‡ Present Address: Department of Chemistry and Chemical Biology, Harvard University, 12 Oxford St., Cambridge, MA 02138.

(1) (a) Pauling, L. *The Nature of the Chemical Bond*; Cornell University Press: Ithaca, NY, 1948. (b) Pimental, G. C.; McClellan, A. L. *The Hydrogen Bond*; W. H. Freeman and Company: San Francisco, CA, 1960. (c) For a fascinating discussion of "Who Discovered the Hydrogen Bond and When", see also Jeffrey, G. A. *An Introduction to Hydrogen Bonding*; Oxford University Press: New York, 1997.

(2) For example, see: (a) Scheiner, S. *Hydrogen Bonding. A Theoretical Perspective*; Oxford University Press: New York, 1997. (b) *Theoretical Treatments of Hydrogen Bonding*; Hadži, D., Ed.; John Wiley and Sons: Chichester, U.K., 1997. (c) *Proton Transfer in Hydrogen-Bonded Systems*; Bountis, T., Ed; NATO ASI Series, Series B: Physics Vol. 291; Plenum: New York, 1992 and references therein.

(3) (a) Coulson, C. A. *Valence*; Oxford University Press: Glasgow, 1952. (b) Mulliken, R. S. *J. Phys. Chem.* **1952**, *56*, 801. (c) Mulliken, R. S.; Person, W. B. *Molecular Complexes. A Lecture and Reprint Volume*; Wiley-Interscience: New York, 1969.

(4) For example, see: Thompson, W. H.; Hynes, J. T. *J. Phys. Chem. A* **2001**, *105*, 2582 and references therein.

(5) For example, see: (a) Redington, R. L, *J. Chem. Phys.* **2000**, *113*, 2319. (b) Tanaka, K.; Honjo, H.; Tanaka, T.; Kohguchi, H.; Ohshima, Y.; Endo, Y. *J. Chem. Phys.* **1999**, *110*, 1969. (c) Luth, K.; Scheiner, S. *J. Phys. Chem*. **1994**, *98*, 3582.

(6) For example, see: (a) Barnes, A. J.; Latajka, Z.; Biczysko, M. *J. Mol. Struct.* **2002**, *614*, 11. (b) Jordan, M. J. T.; Del Bene, J. E. *J. Am. Chem. Soc.* **2000**, *122*, 2101. (c) Hassan, S. A.; Guarnieri, F.; Mehler, E. L. *J. Phys. Chem. B* **2000**, *104*, 6490. (d) Del Bene, J. E.; Jordan, M. J. T. *J. Chem. Phys.* **1998**, *108*, 3205. (e) Lill, M. A.; Hutter, M. C.; Helms, V. *J. Phys. Chem. A* **2000**, *104*, 8283. (f) Del Bene, J. E.; Jordan, M. J. T.; Gill, P. M. W.; Buckingham, A. D. *Mol. Phys.* **1997**, *92*, 429 and references therein.

(7) Ramos, M.; Alkorta, I.; Elguero, J.; Golubev, N. S.; Denisov, G. S.; Benedict, H.; Limbach, H.-H. *J. Phys. Chem. A* **1997**, *101*, 9791.

(8) For example, see: Scheiner, S. *J. Phys. Chem. A* **2000**, *104*, 5898.

(9) For example, see: Hammes-Schiffer, S. *Acc. Chem. Res.* **2001**, *34*, 273.

10.1021/ja030435x CCC: $25.00

methods from NMR to the ultraviolet,[11] as well as mass spectrometry,[12] diffraction techniques,[13] and calorimetry[1c,14] have all been applied, many with substantial support from a wide range of computational methods.[15] There can be little doubt that the abundance of interest in this area reflects its far-reaching relevance in chemistry and biology and that fundamental work on the subject underlies our understanding of numerous natural phenomena.

Among the widely studied prototypes for hydrogen bonding and proton transfer is the class of complexes formed from amines and hydrogen halides. Early experimental work on these systems involved mass spectrometric detection by Goldfinger and Verhaegen,[16] followed shortly thereafter by the well-known matrix infrared studies of Pimentel and others.[17] Subsequent experiments with cryogenic matrixes examined the effects of amine basicity, the identity of the acid, and the nature of the inert matrix on the degree of proton transfer,[18] and indeed a new resurgence of activity has still further developed this line of investigation.[19] Collectively, these studies have shown that the nature of the acid and base, as well as the polarizability of the surrounding medium, combine to give a wide range of complex types in low temperature matrixes, running nearly the full gamut from hydrogen bonds to ion pairs. Thus, for example, H_3N-HF in an argon host is a strongly hydrogen bonded complex,[18c] while $(CH_3)_3N-HBr$ in an N_2 host is better described as a $(CH_3)_3NH^+Br^-$ ion pair.[18g]

For the analogous systems in the gas phase, Legon and coworkers have reported a series of microwave spectroscopic studies[20] on complexes of H_3N, $(CH_3)H_2N$, and $(CH_3)_3N$ with the full set of hydrogen halides and have used nuclear quadrupole coupling constants to estimate the degree of proton transfer in the isolated adducts. Their results showed that although the reaction between NH_3 and any of the hydrogen halides produces an ionic solid under bulk conditions, the isolated 1:1 gas phase complexes, H_3N-HX, are hydrogen bonded and show little or no sign of ion pair formation. As in low temperature matrixes, however, increased methylation of the ammonia and use of the heavier, more acidic hydrogen halides renders ion pair formation observable. Thus, H_3N-HF is a hydrogen bonded system, but the complex formed from $(CH_3)_3N$ and HI is best regarded as a $(CH_3)_3NH^+ I^-$ ion pair, even in the gas phase.

Computationally, the structures and potential energy surfaces for the amine−hydrogen halide complexes have been explored extensively, beginning with work by Clementi[21] and continuing for many years thereafter.[22] Small clusters containing NH_3 and hydrogen halides have also been investigated with an eye toward characterizing the influence of near-neighbor interactions on the transition from hydrogen bonding to ion pairs.[22a,c,e,23] The calculation of observed matrix shifts in the infrared spectra has added yet another dimension to the computational work in this area, providing a direct complement to the matrix infrared experiments and demonstrating the need for proper description of anharmonicity in the quantitative determination of matrix interactions.[24]

One of the many interesting issues arising in the study of the amine−hydrogen halide systems, and indeed proton transfer in general, involves the effect of a surrounding medium on the relative stabilities of the hydrogen bonded and proton-transferred forms. Although a variety of approaches have been explored to treat this problem, it remains a topic of discussion, even today, as to when a discrete representation of the surrounding medium is preferable to a less realistic but computationally simpler continuum model.[25] In this context, therefore, it is of interest to investigate the effect of a single near-neighbor on the nature

(10) For example, see: (a) Remer, L. C.; Jensen, J. H. *J. Phys. Chem. A* **2000**, *104*, 9266. (b) Kim, Y.; Lim, S.; Kim, Y. *J. Phys. Chem. A* **1999**, *103*, 6632. (c) Madsen, G. K. H.; Wilson, C.; Nymand, T. M.; McIntyre, G. J.; Larsen, F. K. *J. Phys. Chem. A* **1999**, *103*, 8684. (d) Perrin, C. L.; Nielson, J. B. *Annu. Rev. Phys. Chem.* **1997**, *48*, 511.

(11) For example, see: (a) *Magn. Reson. Chem.* **2001**, *39*, S1−S2, entire issue. (b) Bagno, A.; Scorrano, G. *Acc. Chem. Res.* **2000**, *33*, 609. (c) Zwier, T. S. *Annu. Rev. Phys. Chem.* **1996**, *47*, 205. (d) Pratt, D. W. *Annu Rev. Phys. Chem.* **1998**, *49*, 481. (e) Ebata, T.; Fujii, A.; Mikami, N. *Int. Rev. Phys. Chem.* **1998**, *17*, 331. (f) Ayoette, P.; Weddle, G. H.; Bailey, C. G.; Johnson, M. A.; Vila, F.; Jordan, K. D. *J. Chem. Phys.* **1999**, *110*, 6268. (g) Bieske, E. J.; Dopfer, O. *Chem. Rev.* **2000**, *100*, 3963. (h) Devlin, J. P.; Sadley, J.; Buch, V. *J. Phys. Chem. A* **2001**, *105*, 974. (i) Neusser, H. J.; Siglow, K. *Chem. Rev.* **2000**, *100*, 3921. (j) Dessent, C. E. H.; Müller-Dethlefs, K. *Chem. Rev.* **2000**, *100*, 3999. (k) Liu, K.; Brown, M. G.; Saykally, R. J. *J. Phys. Chem. A* **1997**, *101*, 8995. (l) Lisy, J. M. *Int. Rev. Phys. Chem.* **1997**, *16*, 267. (m) Leopold, K. R.; Fraser, G. T.; Novick, S. E.; Klemperer, W. *Chem. Rev.* **1994**, *94*, 1807 and references therein.

(12) For example, see: (a) *Gas-Phase Ion Chemistry, Vol. 2*; Bowers, M. T., Ed.; Academic Press: New York, 1979. (b) Gal, J.-F.; Maria, P.-C. *Prog. Phys. Org. Chem.* **1990**, *17*, 159. (c) Hunter, E. P.; Lias, S. G. Proton Affinity Evaluation. In *NIST Chemistry WebBook, NIST Standard Reference Database Number 69*; Linstrom, P. J.; Mallard, W. G., Eds.; March 2003, National Institute of Standards and Technology, Gaithersburg, MD, 20899 (http://webbook.nist.gov). (d) Wolf, J. F.; Staley, R. H.; Koppel, I.; Taagepera, M.; McIver, R. T., Jr.; Beauchamp, J. L. Taft, R. W. *J. Am. Chem. Soc.* **1977**, *99*, 5417. (e) Sugai, T.; Shinohara, H. *Chem. Phys. Lett.* **1997**, *264*, 327 and references therein.

(13) For example, see: (a) Hargittai, M.; Hargittai, I. *The Molecular Geometries of Coordination Compounds in the Vapor Phase*; Elsevier: Amsterdam, 1977. (b) Bürgi, G. B.; Dunitz, J. D. *Acc. Chem. Res.* **1983**, *16*, 153. (c) Taylor, R.; Kennard, O. *Acc. Chem. Res.* **1984**, *17*, 320. (d) Taylor, R.; Kennard, O. *J. Am. Chem. Soc.* **1982**, *104*, 5063. (e) Etter, M. C. *J. Phys. Chem.* **1991**, *95*, 4601. (f) Shibata, S. *Acta Chem. Scand.* **1970**, *24*, 705 and references therein.

(14) For example, see: (a) Joesten, M. D.; Schaad. L. J. *Hydrogen Bonding*; Marcel Dekker: New York, 1974; (b) Arnett, E. M.; Joris, L.; Mitchell, E.; Murty, T. S. S. R.; Gorrie, T. M. Schleyer, P. v. R. *J. Am. Chem. Soc.* **1970**, *92*, 2365.

(15) For example, see: (a) Del Bene, J. E.; Shavitt, I. In *Molecular Interactions from van der Waals to Strongly Bound Complexes*; Scheiner, S., Ed.; Wiley: New York, 1997. (b) Gordon, M. S.; Jensen, J. H. *Acc. Chem. Res.* **1996**, *29*, 536. (c) Hobza, P.; Havlas, Z. *Chem. Rev.* **2000**, *100*, 4253. (d) Scheiner, S. *Acc. Chem. Res.* **1994**, *27*, 402 and references therein.

(16) Goldfinger, P.; Verhaehen, G. *J. Chem. Phys.* **1969**, *50*, 1467.

(17) (a) Ault, B. S.; Pimentel, G. C. *J. Phys. Chem.* **1973**, *77*, 1649. (b) Ault, B. S.; Steinback, E.; Pimentel, G. C. *J. Phys. Chem.* **1975**, *79*, 615. (c) Barnes, A. J.; Orville-Thomas, W. J. *J. Mol. Spectrosc.* **1978**, *45*, 75.

(18) For example, see: (a) Barnes, A. J.; Szczepaniak, K.; Orville-Thomas, W. J. *J. Mol. Struct.* **1980**, *59*, 39. (b) Barnes, A. J. *J. Mol. Struct.* **1980**, *60*, 343. (c) Johnson, G. L.; Andrews, L. *J. Am. Chem. Soc.* **1982**, *104*, 3043. (d) Schriver, L.; Schriver, A.; Perchard, J. P. *J. Am. Chem. Soc.* **1983**, *105*, 3843. (e) Barnes, A. J.; Beech, T. R.; Mielke, Z. *J. Chem. Soc., Faraday Trans. 2* **1984**, *80*, 455. (f) Barnes, A. J.; Kuzniarski, J. N. S.; Mielke, Z. *J. Chem. Soc., Faraday Trans. 2* **1984**, *80*, 465. (g) Barnes, A. J.; Wright, M. P. *J. Chem. Soc., Faraday Trans. 2* **1986**, *82*, 153. (h) Andrews, L.; Davis, S. R.; Johnson, G. L. *J. Phys. Chem.* **1986**, *90*, 4273.

(19) (a) Andrews, L.; Wang, X. *J. Phys. Chem. A* **2001**, *105*, 6420. (b) Andrews, L.; Wang, X.; Mielke, Z. *J. Am. Chem. Soc.* **2001**, *123*, 1499. (c) Andrews, L.; Wang, X.; Mielke, Z. *J. Phys. Chem. A* **2001**, *105*, 6054. (d) Andrews, L.; Wang, X. *J. Phys. Chem. A* **2001**, *105*, 7541. (e) Barnes, A. J.; Legon, A. C. *J. Mol. Struct.* **1998**, *448*, 101.

(20) Legon, A. C. *Chem. Soc. Rev.* **1993**, 153 and references therein.

(21) Clementi, E. *J. Chem. Phys.* **1967**, *46*, 3851.

(22) For example, see: (a) Cherng, B.; Tao, F.-M. *J. Chem. Phys.* **2001**, *114*, 1720. (b) Tao, F.-M. *J. Chem. Phys.* **1999**, *110*, 11121. (c) Heidrich, D. *THEOCHEM* **1998**, *429*, 87. (d) Corongiu, G.; Estrin, D.; Murgia, G.; Paglieri, L.; Pisani, L.; Valli, G. S.; Watts, J. D.; Clementi, E. *Int. J. Quantum Chem.* **1996**, *59*, 119. (e) Heidrich, D.; van Eikema Hommes, J. R.; Schleyer, P. v. R. *J. Comput. Chem.* **1993**, *14*, 1149. (f) Latajka, Z.; Scheiner, S.; Ratajczak, H. *Chem. Phys. Lett.* **1987**, *135*, 367. (g) Brciz, A.; Karpfen, A.; Lischka, H.; Schuster, P. *Chem. Phys.* **1984**, *89*, 337.

(23) (a) Chaban, G. M.; Gerber, R. B.; Janda, K. C. *J. Phys. Chem. A* **2001**, *105*, 8323. (b) Snyder, J. A.; Cazar, R. A.; Jamka, A. J.; Tao, F.-M. *J. Phys. Chem. A* **1999**, *103*, 7719. (c) Biczysko, M.; Latajka, Z. *Chem. Phys. Lett.* **1999**, *313*, 366.

(24) (a) Barnes, A. J.; Latajka, Z.; Biczysko, M. *J. Mol. Struct.* **2002**, *614*, 11. (b) Bevitt, J.; Chapman, K.; Crittenden, D.; Jordan, M. J. T.; Del Bene, J. E. *J. Phys. Chem. A* **2001**, *105*, 3371. (c) Jordan, M. J. T.; Del Bene, J. E. *J. Am. Chem. Soc.* **2000**, *122*, 2101. (d) Del Bene, J. E.; Jordan, M. J. T. *J. Chem. Phys.* **1998**, *108*, 3205. (e) Del Bene, J. E.; Jordan, M. J. T.; Gill, P. M. W.; Buckingham, A. D. *Mol. Phys.* **1997**, *92*, 429.

of a hydrogen bonded complex. Several workers have studied the effect of an additional HF molecule on the structure and bonding of H_3N-HF, both theoretically[22c,e] and in cryogenic matrixes,[18c] and a number of computational papers have addressed the effect of additional water molecules.[23b,c] The complexes of methylated amines with two HF moieties have also been investigated by matrix infrared spectroscopy.[18h] However, while these studies have shown that matrixes and small clusters can indeed advance the degree of proton transfer in some cases, we are unaware of any gas phase studies that have definitively quantified these effects by high-resolution spectroscopic techniques. In this work, therefore, we investigate the effect of a single, polar near-neighbor on the extent of proton transfer in a simple hydrogen bonded complex, reporting rotational spectroscopy, as well as ab initio energy and structure calculations, on the complex $H_3N-HF-HF$. Additionally, for the purpose of providing a careful comparison, we apply the same techniques to improve on a previous preliminary report on the structure of the H_3N-HF dimer.[20,26] Together, these studies provide a rather complete characterization of the H_3N-HF hydrogen bond and of the extent to which microsolvation promotes measurable change in the degree of proton transfer across it.

Experimental Methods and Results

The rotational spectra of H_3N-HF and $H_3N-HF-HF$ and their isotopomers were recorded using the pulsed-nozzle Fourier transform microwave technique originally developed by Balle and Flygare.[27] Details of our spectrometer have been described elsewhere.[28] Briefly, molecules enter a microwave cavity evacuated by a 20 000 L/s diffusion pump and are irradiated with a 2 μs pulse of microwave radiation. Molecular transitions within the spectral bandwidth of the radiation are coherently excited, and the resulting free induction decay is heterodyne detected, signal averaged, and Fourier transformed to produce a spectrum in the frequency domain. The spectrometer covers a spectral range nominally between 3 and 18 GHz, over which individual transition frequencies are typically recorded with an estimated uncertainty of about 3 kHz.

Both H_3N-HF and $H_3N-HF-HF$ were produced in a supersonic expansion, with an injection source similar to that used previously for other reactive systems.[29] Optimum signals were obtained by pulsing a mixture of 0.5% NH_3 in argon through a 0.8 mm nozzle orifice with a backing pressure of 2 atm. Neat HF flowing at a rate of 5 standard cm^3/min was introduced into the expansion approximately 0.17″ below the nozzle orifice through a 0.010″ inner diameter stainless steel needle with a 90° bend to direct the HF along the axis of the expansion. Attempts to pulse an Ar/HF mixture and introduce neat ammonia through the needle resulted in substantially poorer signals. For deuterated species, 99 atom % ND_3 or 99 atom % DF (both obtained from Icon Services) were used, as appropriate, and the ^{15}N-containing isotopomer of H_3N-HF was observed in natural abundance. Although NH_3 and HF react to form a solid, significant build-up of the solid on the needle tip was not observed and experimental conditions were quite stable over time.

Table 1. Spectroscopic Constants for H_3N-HF and Its Isotopic Dervatives[a]

	B_{eff}[b] (MHz)	χ_N (MHz)	D_{aa} (kHz)
H_3N-HF	7366.0326(48)	−3.334(20)	
H_3N-DF	7347.1421(76)	−3.316(33)	
D_3N-HF	6450.7708(91)	−3.465(37)	
D_3N-DF	6428.4267(65)	−3.429(27)	
$H_3{}^{15}N-HF$	7173.4373(13)		−251.1(93)

[a] Numbers in parentheses are one standard error in the least-squares fits. [b] $B_{eff} \equiv B - 2D_J$, where D_J is the centrifugal distortion constant.

For H_3N-HF, the $J = 1 \leftarrow 0$ rotational transition was readily located using the previously reported N···F distance,[20,26] and spectra were subsequently recorded for five isotopic forms. Transitions corresponding to higher values of J lie far outside the spectral range of our instrument and were not observed. Thus, only $B_{eff} \equiv B - 2D_J$ (where B is the rotational constant and D_J is the centrifugal distortion constant) is determined from the spectrum. The ammonia inversion motion is quenched in the system, and the complex is a symmetric top. Thus, no additional transitions are expected in this range. Hyperfine structure due to both the ^{14}N nuclear quadrupole interaction and the HF spin−spin interaction (in $^{15}NH_3-HF$) was observed and analyzed according to standard methods[30] to give the nitrogen nuclear quadrupole coupling constant (χ_N) and the HF spin−spin interaction constant (D_{HF}). Spectroscopic constants are given in Table 1, and spectral frequencies are provided as Supporting Information.

For $H_3N-HF-HF$, the spectra were considerably more complicated and confirmed the expectation that the molecule is an asymmetric rotor with hindered internal rotation of the NH_3 unit about its C_3 axis. Accordingly, two sets of spectra were observed, one corresponding to no internal rotation of the ammonia (A state) and one corresponding to molecules with internally rotating NH_3 (E state). These correlate with free ammonia in its $K = 0$ and $K = \pm 1$ states, respectively, which are themselves associated with differing proton nuclear spin functions. Since cooling in the jet does not readily interconvert nuclear spin states, the E state remains populated despite its approximately 6.2 cm^{-1} of additional energy. Only a single excited internal rotation state was observed in these experiments.

Because of the complexity of the spectrum, nearly 12 GHz were scanned (in 625 kHz steps) in order to obtain firm assignments for the parent species. Figure 1 contains a stick spectrum of transitions observed, and Figure 2 provides a sample spectrum showing the three ^{14}N nuclear hyperfine components in the $1_{01} \leftarrow 0_{00}$ transition of the E state. A detailed listing of transition frequencies for all isotopic forms of the trimer observed is also given in the Supporting Information. As seen in Figure 1, the spectrum of this complex includes several pairs of transitions with internal rotation splittings ranging from 56 to 566 MHz. Initial assignments were based on the identification of two closed energy loops, each including four transitions, and preliminary spectral fits for the A state using a standard rigid rotor plus Watson's A-reduced Hamiltonian for centrifugal distortion[31] yielded satisfactory results. However, since the energy levels of the excited internal rotor state are perturbed by internal rotation, the preliminary fit for the E state data gave unreasonably large distortion constants (on the order of tens of MHz) and large residuals in the individual hyperfine components. A phenomenological approach employing effective quadrupole coupling constants for each rotational energy level was initially taken to resolve

(25) (a) Milischuk, A.; Matyushov, D. V. *J. Chem. Phys.* **2003**, *118*, 1859. (b) Shoeib, T.; Ruggiero, G. D.; Siu, K. W. M.; Hopkinson, A. C.; Williams, I. H. *J. Chem. Phys*. **2002**, *117*, 2762. (c) Cossi, M.; Scalmani, G.; Rega, N.; Barone, V. *J. Chem. Phys.* **2002**, *117*, 43. (d) Aquino, A. J. A.; Tunega, D.; Haberhauer, G.; Gerzabek, M. H.; Lischka, H. *J. Phys. Chem. A* **2002**, *106*, 1862. (e) Cossi, M.; Barone, V. *J. Chem. Phys.* **2000**, *112*, 2427. (f) Hassan, S. A.; Guarnieri, F.; Mehler, E. L. *J. Phys. Chem. B* **2000**, *104*, 6490. (g) Abkowicz-Bienko, A.; Biczysko, M.; Latajka, Z. *Comput. Chem.* **2000**, *24*, 303. (h) Gao, J. *Acc. Chem. Res.* **1996**, *29*, 298.
(26) Howard, B. J.; Langridge-Smith, P. R. R., quoted in Howard, B. J.; Legon, A. C. *J. Chem. Phys.* **1987**, *86*, 6722.
(27) Balle, T. J.; Flygare, W. H. *Rev. Sci. Instrum*. **1981**, *52*, 33.
(28) (a) Phillips, J. A.; Canagaratna, J.; Goodfriend, H.; Grushow, A.; Almlöf, J.; Leopold, K. R. *J. Am. Chem. Soc.* **1995**, *117*, 12549. (b) Phillips, J. A. Ph.D. Thesis, University of Minnesota, 1996.
(29) (a) Canagaratna, M.; Phillips, J. A.; Goodfriend, H.; Leopold, K. R. *J. Am. Chem. Soc.* **1996**, *118*, 5290. (b) Legon, A. C.; Wallwork, A. L.; Rego, C. A. *J. Chem. Phys*. **1990**, *92*, 6397. (c) Gillies, C. W.; Gillies, J. Z.; Suenram, R. D.; Lovas, F. J.; Kraka, E.; Cremer, D. *J. Am. Chem. Soc*. **1991**, *113*, 2412.
(30) Townes, C. H.; Schawlow, A. *Microwave Spectroscopy*; Dover: New York, 1975.
(31) Watson, J. K. G. *J. Chem. Phys.* **1967**, *46*, 1935.

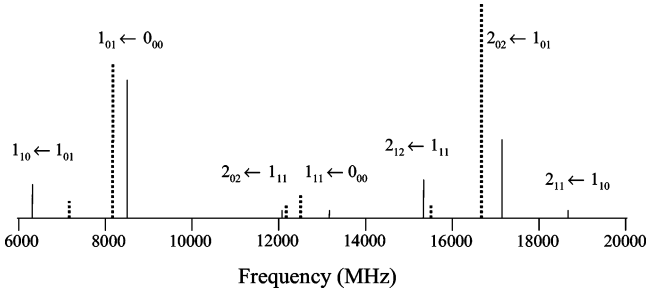

Figure 1. Stick spectrum indicating observed transitions for $^{14}NH_3-HF-HF$. Solid lines correspond to transitions of the A state, and dotted lines correspond to those of the E state. The $2_{11} \leftarrow 2_{02}$ transition of the A state was also measured but is not shown in this figure, as it lies very close to the $1_{01} \leftarrow 0_{00}$ transition. Relative intensities are indicated as they were observed on our apparatus but do not reflect the intrinsic strength of the transitions due to variability of instrumental sensitivity throughout the accessible spectral range.

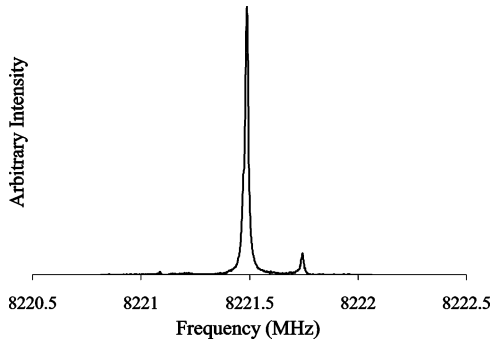

Figure 2. High-resolution trace showing ^{14}N hyperfine components in the $1_{01} \leftarrow 0_{00}$ transition of the E state of $H_3N-HF-HF$. This spectrum represents 43 s of data collection time.

these difficulties, and this indeed provided confirmation of the assignments as well as a much improved fit for the E state (residuals typically less than 7 kHz). However, even with this method of analysis, separate fitting of the two internal rotor states yields only *effective* rotational constants, which do not directly give the inverse moments of inertia of the complex (even for the A state). Furthermore, the splittings between the A and E internal rotor state lines contain information about the barrier to internal rotation of the ammonia that cannot be utilized by treating the two states separately. Thus, a simultaneous analysis of spectral data for both internal rotor states was undertaken.

The combined analysis of both internal rotor states was accomplished using the program XIAM by Hartwig and Dreizler,[32] which is available at the Programs for Rotational Spectroscopy website.[33] This program uses the internal axis method, which was originally given by Woods[34,35] and modified by Vacherand[36] and has also been referred to as the combined axis method (CAM). Briefly, the Hamiltonian is written

$$H = H_r + H_{cd} + H_{ir} + H_{ird} + H_Q \quad (1)$$

where H_r is the usual Hamiltonian for an asymmetric rotor, and H_{cd} is the Watson, A-reduced Hamiltonian for centrifugal distortion.[31] H_{ir} is the internal rotation Hamiltonian, which may be written

$$H_{ir} = F(\mathbf{p}_\alpha - \rho\cdot\mathbf{P})^2 + V(\alpha) \quad (2)$$

where α is the internal rotation angle for the NH_3 group. $\mathbf{p}_\alpha$ in this expression is given as

$$\mathbf{p}_\alpha = -i(\partial/\partial\alpha) \quad (3)$$

and F is the internal rotation constant for an internal rotor with moment of inertia I_α, viz.

$$F = h^2/2rI_\alpha \quad (4)$$

where

$$r = 1 - \sum_g \lambda_g^2\left(\frac{I_\alpha}{I_g}\right) = 1 - \lambda_a^2\left(\frac{I_\alpha}{I_a}\right) - \lambda_b^2\left(\frac{I_\alpha}{I_b}\right) \quad (5)$$

The second equality in eq 5 arises because the NH_3 rotor is in the $a-b$ plane of the complex. ρ, in eq 2, is a vector, whose components are

$$\rho_g = \lambda_g(I_\alpha/I_g) \quad (6)$$

where I_g is the moment of inertia of the complex about its g-inertial axis, I_α is the moment of inertia of the ammonia top about the internal rotation axis, and λ_g is the direction cosine between the internal rotation axis and the g-inertial axis of the complex. The potential function for internal rotation, $V(\alpha)$, was truncated at the 3-fold barrier term to give

$$V(\alpha) = {}^1/_2V_3[1 - \cos(3\alpha)] \quad (7)$$

H_{ird}, given elsewhere,[33,37] contains a number of distortion terms that arise due to internal rotation. Finally, H_Q has the usual form describing the nuclear quadrupole coupling in an asymmetric top and was included to analyze hyperfine structure due to the ^{14}N nucleus, when present. Note that the principal axes of the inertial and quadrupole coupling tensors of this complex do not coincide and hence χ_{ab}, the off -diagonal element of the quadrupole coupling tensor, is nonzero. However, since the c-axis is perpendicular to the symmetry plane of the complex, the cross terms χ_{ac} and χ_{bc} are still zero. The effect of χ_{ab} becomes particularly important in the spectrum of the E state, where the interaction of the internal rotation with the overall rotation results in a mixing of levels of even and odd K, making $\langle \mathbf{P}_a\mathbf{P}_b + \mathbf{P}_b\mathbf{P}_a\rangle$ nonzero.[38]

In XIAM, the Hamiltonian is defined in the principal axis system. Matrix elements of H_{ir}, however, are first calculated in the "ρ-axis system" and transformed into the principal axis system by appropriate axis rotation, as described elsewhere.[33-36] We note here only that since the components of the vector ρ depend on the direction cosines between the internal rotation axis and the principal axes, the Hamiltonian also implicitly contains a parameter,

$$\cos\delta \equiv \lambda_a = \rho_a(I_a/I_\alpha) \quad (8)$$

where δ is the angle between the internal rotation axis and the a-inertial axis of the complex.

Individual fits for each of the seven isotopomers of $H_3N-HF-HF$ studied were performed with XIAM using this method. A listing of the results, including rotational constants and the 3-fold internal rotation barrier, is given in Table 2. Note that the linear combinations $(B + C)/2$, $[A - (B + C)/2]$, and $(B - C)/2$ were fit, rather than A, B, and C, to minimize correlation. Although each of the seven isotopomers studied were independently analyzed, measurement of fewer transitions for the species including deuterium required fixing several values at the results obtained for the parent species, as indicated in the table. For example, while the internal rotation barrier, V_3, was determined independently for $NH_3-HF-HF$, $ND_3-HF-HF$, and

(32) Hartwig, H.; Dreizler, H. *Z. Naturforsch.* **1996**, *51a*, 923.
(33) The Programs for Rotational Spectroscopy website may be found at http://info.ifpan.edu.pl/~kisiel/prospe.htm.
(34) Woods, R. C. *J. Mol. Spectrosc.* **1966**, *21*, 4.
(35) Woods, R. C. *J. Mol. Spectrosc.* **1967**, *22*, 49.
(36) Vacherand, J. M.; Eijck, B. P. v.; Burie, J.; Demaison, J. *J. Mol Spectrosc.* **1986**, *118*, 355.
(37) Hunt, S. W. Ph.D. Thesis, University of Minnesota, 2002.
(38) Fraser, G. T.; Suenram, R. D.; Lovas, F. J. *J. Chem. Phys.* **1987**, *86*, 3107.

Table 2. Spectroscopic Constants of NH_3−HF−HF and Its Isotopic Derivatives[a]

	NH_3–HF–HF	NH_3–DF–HF	NH_3–HF–DF	ND_3–HF–HF	ND_3–DF–HF	ND_3–HF–DF	ND_3–DF–DF
$(B+C)/2$	4225.9134(18)	4191.8800(31)	4177.4892(45)	3856.5137(44)	3819.94(24)	3811.482(45)	3774.7138(55)
$[A-(B+C)/2]$	5420.5401(36)	5130.276[b]	5384.072[b]	4984.8215(96)	4682.9[b]	5025.7[b]	4994.816[b]
$(B-C)/2$	858.0602(35)	863.505(12)	847.113(19)	746.3302(64)			722.6710(74)
Δ_J	0.076 00(33)	0.076 02(96)	0.0760(11)	0.047 27(48)	0.072 50[b]	0.072 50[b]	0.072 50(52)
Δ_{JK}	−0.3756(13)	−0.3756[b]	−0.3756[b]	−0.3004(21)	−0.3756[b]	−0.3756[b]	−0.3756[b]
δ_J	0.029 28(28)	0.029 28[b]	0.029 28[b]	0.02928[b]	0.029 28[b]	0.029 28[b]	0.029 28[b]
χ_{aa}	0.6740(49)	0.6516(93)	0.707(15)	0.3876(89)	0.398(32)	0.397(33)	0.400(11)
$\chi_{bb}-\chi_{cc}$	−3.949(12)	−3.855(74)	−4.02(16)	−3.810(31)	−3.72(35)	−3.36(40)	−4.027(74)
χ_{ab}	−1.802(36)	−1.802[b]	−1.802[b]	−1.802[b]	−1.802[b]	−1.802[b]	−1.802[b]
$\Delta_{\pi^2 J}$	5.9552(53)	5.9552[b]	5.9552[b]	4.704(33)	3.04(96)	3.6(11)	4.709(37)
$\Delta_{\pi^2 K}$	−17.462(19)	−17.462[b]	−17.462[b]	−17.462[b]	−17.462[b]	−17.462[b]	−17.462[b]
Δ_{π^2}	3.4336(67)	3.4336[b]	3.4336[b]	3.4336[b]	3.4336[b]	3.4336[b]	3.4336[b]
V_3 [cm^{-1}]	117.5818(13)	117.5818[b]	117.5818[b]	119.910(32)	119.910[b]	119.910[b]	117.823(27)
δ[c] [degrees]	117.0774(9)	117.0774[b]	117.0774[b]	120.81(2)	124.2(27)	124.1(25)	120.99(4)
N_{lines}[d]	53	9	9	31	11	11	26

[a] All values in MHz, unless noted. [b] Held fixed. See text for details. [c] Defined in eq 8. [d] Number of transitions included in the fit.

ND_3−DF−DF, searches were not conducted for the E states of NH_3−HF−DF and NH_3−DF−HF. Thus, parameters related to the internal rotation were fixed at values for the parent isotopomer. Note that the agreement among the three independent determinations of V_3 is excellent.

In obtaining the results in Table 2, several additional procedures were required due to the details and scope of the individual isotopic data sets. For instance, the $1_{01} \leftarrow 0_{00}$ transition of the A state of ND_3−HF−DF and the $1_{01} \leftarrow 0_{00}$ transition of the E state of ND_3−DF−HF were separated by less than 1 MHz, and consequently, their assignments were somewhat ambiguous. The assignments used are those that resulted in the best fit of the hyperfine structure. However, since the residuals of the fits employing either assignment vary by only a few kHz, spectroscopic constants given for these two species are an average of those resulting from the two possibilities, with combined error bars. These fits were performed with V_3 held fixed at both the values fitted for the ND_3−HF−HF and ND_3−DF−DF species, and while differences in the fits were small, the best fit, as judged by the residuals, was obtained using the barrier height determined with the ND_3−HF−HF data. Also, since b-type transitions were only observed for the NH_3−HF−HF and ND_3−HF−HF species, the term $[A-(B+C)/2]$ was not well determined for the other species. Because of the strong dependence of the spectrum on $\kappa \equiv (2B-A-C)/(A-C)$, fixing $[A-(B+C)/2]$ at the values based on theoretical isotope shifts resulted in poor fits and a wide range of values of Δ_J. Therefore, a preliminary set of fits was performed while freeing $[A-(B+C)/2]$, and then the determined values were held fixed in the final fits. Finally, since only $K_p = 0$ transitions were measured for D_3N−HF−DF and D_3N−DF−HF, $(B-C)/2$ is not determined or included in the fits. In all other cases where spectroscopic constants are not determined, they were fixed at values obtained for the parent species. Further details are given elsewhere.[37]

Structure Analysis

H_3N−HF. The observed rotational constants of H_3N−HF are near those predicted on the basis of the NF distance previously quoted as unpublished work.[20,26] The data are consistent with a symmetric top structure with the HF hydrogen directed toward the lone pair on the ammonia, as in other H_3N−HX (X = Cl, Br, I) dimers as well as in the theoretical structure of H_3N−HF.[22c,e,23b,24d,25g] The observed rotational constants of the complex were analyzed using the coordinates defined in Figure 3a, where the angles σ and τ are included to account for large amplitude angular vibration of the NH_3 and HF, respectively, and R_{cm} is the distance between the centers of mass of the monomers. In terms of these coordinates, the moment of inertia

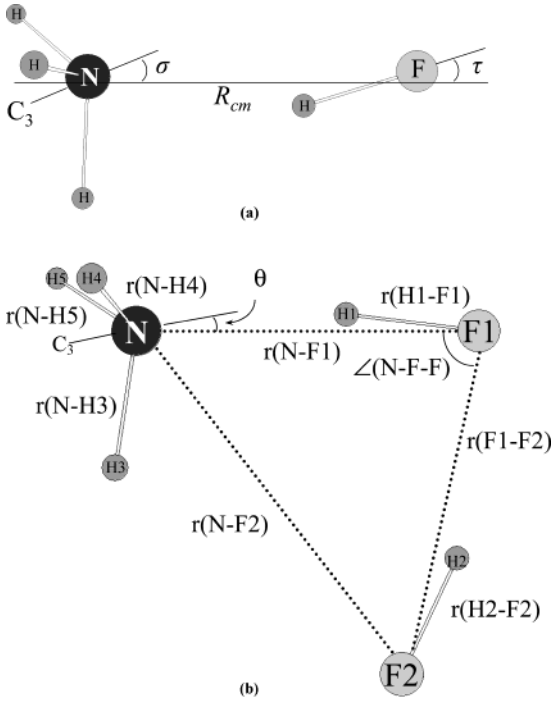

Figure 3. (a) Definition of coordinates used to describe the structure of H_3N−HF. σ and τ describe angular vibrations about an equilibrium C_{3v} geometry. (b) Definition of coordinates and atom labeling for H_3N−HF−HF. The angle, θ, between the C_3 axis of the NH_3 and the line joining N and F1 is shown as a positive value.

of the complex about the *b*-inertial axis, $\langle I_{bb}\rangle = h/8\pi^2 B$, can be written

$$\langle I_{bb}\rangle = M_s\langle R_{cm}^2\rangle + {}^1/_2 I_{bb}(NH_3)[1+\langle\cos^2\sigma\rangle] + {}^1/_2 I_{cc}(NH_3)\langle\sin^2\sigma\rangle + {}^1/_2 I_{bb}(HF)[1+\langle\cos^2\tau\rangle] \quad (9)$$

where $M_s = m(NH_3)m(HF)/m(H_3N-HF)$, the I_{gg}'s are the moments of inertia of the indicated units about their *g*-inertial axes, and the angular brackets denote averaging over the ground vibrational state wave function. The moments of inertia of the NH_3 and HF were assumed in eq 9 to equal those of free NH_3[39] and free HF,[40] which should be a reasonable approximation since the complex is weakly bound, and since the last three terms

(39) Helminger, P.; De Lucia, F. C.; Gordy, W. *J. Mol. Spectrosc.* **1971**, *39*, 94.
(40) Guelachvili, G. *Opt. Commun.* **1976**, *19*, 150.

provide relatively small corrections to $M_s\langle R_{cm}^2\rangle$. However, due to the possibility of partial proton transfer across the hydrogen bond, a modest elongation of the HF bond was also considered and its effects incorporated into the analysis, as described below.

Values of $\langle\cos^2\sigma\rangle$ and $\langle\cos^2\tau\rangle$ were estimated from the observed nuclear hyperfine structure assuming that the observed hyperfine constants in the complex are the tensor projections of the free-molecule values onto the *a*-inertial axis of the dimer, viz.

$$\chi_N(H_3N{-}HF) = (^1/_2)\chi_N(H_3N)\langle 3\cos^2\sigma - 1\rangle \quad (10a)$$

and

$$D_{HF}(H_3N{-}HF) = (^1/_2)D_{HF}(HF)\langle 3\cos^2\tau - 1\rangle \quad (10b)$$

Using the measured ^{14}N quadrupole coupling constant for each isotopomer of $H_3N{-}HF$ and the value for that of free ammonia ($-4.089\,83(2)$ MHz[41]),eq 10a results in values for $\sigma_{eff} \equiv \cos^{-1}[\langle\cos^2\sigma\rangle^{1/2}]$ ranging from 18.6° to 20.8°. These values are not unreasonable for weakly bound ammonia, though we note that, with the possibility of electronic rearrangement at the nitrogen, the true values could lie somewhat outside this range. The correction for possible electronic contributions is difficult to estimate, and thus, we report an approximate value of $\sigma_{eff} = 20°$, with a somewhat arbitrary uncertainty of about 2°. Similarly, using the measured spin−spin coupling constant, D_{HF}, and the value for that in free HF ($-286.75(5)$ kHz[42,43]), eq 10b gives a value of $\tau_{eff} \equiv \cos^{-1}[\langle\cos^2\tau\rangle^{1/2}] = 17(3)°$. Here, the 3° uncertainty is large enough to encompass that arising from the measurement of D_{HF}. A value of 17° appears quite reasonable as it is just a few degrees larger than the 14° value previously estimated for the more tightly bound $(CH_3)_3N{-}HF$.[44]

It should be noted that the above analysis of D_{HF} assumes that its reduction relative to that in free HF arises entirely from angular motion. In a study of $(CH_3)_3N{-}HF$, however, Legon and Rego[44] have pointed out that since D_{HF} varies inversely with r_{HF}^3, the measured value may also reflect a lengthening of the HF bond. Indeed, according to the MP2/aug-cc-pVTZ (CP) counterpoise-corrected geometries reported below, the HF distance increases by 0.034 Å upon complexation with ammonia. Although the lack of an independent measure of τ_{eff} for $H_3N{-}HF$ precludes an experimental determination of this value, an upper limit can be obtained assuming that angular motion makes *no* contribution to D_{HF}, that is, $\tau_{eff} = 0$. In this limit, using a value of the HF bond length in free HF equal to 0.925 595 Å,[40] and assuming that $D_{HF} \propto 1/r_{HF}^3$, the change in HF bond length, δr_{HF}, is determined to be 0.041 Å. The value is quite reasonable, as it is slightly higher than the ab inito value (as an upper limit should be). Moreover, previous work on $(CH_3)_3N{-}HF$, where an independent estimate of τ_{eff} was available, also gave $\delta r_{HF} = 0.041$ Å.[44] Since the interaction is presumably stronger with the more basic amine, our upper limit of $\delta r_{HF} = 0.041$ Å for $H_3N{-}HF$ is sensible and the ab initio value of 0.034 Å is probably quite realistic. Certainly, the observed value of D_{HF} results from a combination of *both* a lengthening of the HF bond and angular excursion of the HF unit.

Table 3. Structural Parameters for $H_3N{-}HF$

parameter	value
R_{cm} [Å][a]	2.6800(13)
R(N···F) [Å]	2.640(21)
R(N···H) [Å]	1.693(42)
σ_{eff} [degrees]	20(2)
τ_{eff} [degrees]	17(3)

[a] Value for the parent isotopomer, $H_3{}^{14}N{-}HF$.

Using the values of τ_{eff} obtained from D_{HF} and σ_{eff} determined from the ^{14}N data, R_{cm} was calculated for each isotopomer from the measured rotational constant.[45] Assuming that the HF bond length is unchanged relative to that in free HF results in values of R_{NF} ranging from 2.6195 to 2.6613 Å, and if the HF bond distance is increased by 0.041 Å, the values of R_{NF} are only approximately 0.0010 Å longer. Because of the uncertainty associated with the HF excursion, values of R_{cm} were also calculated with $\tau_{eff} = 0°$, and again the results differed by less than 0.001 Å. The final value of R_{cm} for the parent species, including these variations, is 2.6800(13) Å, and from all isotopomers, R_{NF} is 2.640(21) Å. Assuming the HF distance is equal to that in the free monomer, the hydrogen bond length is 1.714 Å, and this distance decreases to 1.673 Å if the HF bond lengthens by 0.041 Å. The "preferred" value, therefore. is reported as 1.693(42) Å. These results are summarized in Table 3.

$H_3N{-}HF{-}HF$. Determination of the structure of $H_3N{-}HF{-}HF$ was significantly more complicated than that for the dimer. The spectroscopic constants are indicative of a reasonably asymmetric top, with Ray's asymmetry parameter, $\kappa = -0.453$ for the parent isotopomer, and since all atoms have not been isotopically substituted, it was necessary to hold several parameters fixed in the structure determination. The geometry of the trimer was defined in terms of the separation of the three heavy atoms as indicated in Figure 3b, where the C_3 axis of the NH_3 makes an angle θ with the line connecting N and F1. The HF bonds were allowed to deviate from the lines connecting the heavy atoms, as indicated. Although theoretical calculations indicate that the equilibrium structure of the complex has a planar $HN{-}HF{-}HF$ ring, possible departures of the ring structure from planarity were also considered in the analysis.

Typically, for weakly interacting species, parameters within the monomer units can be assumed to equal their values in the free species. However, because of the relatively strong interactions within this complex, it is not necessarily appropriate to constrain the NH_3 and HF units to their free-molecule geometries. The highest level theoretical calculation described in the following section shows that, in $H_3N{-}HF{-}HF$, the inner and outer HF bond distances elongate by 0.07 and 0.02 Å, respectively, relative to those in free HF. Changes within the NH_3 unit are also discernible but smaller in magnitude. Therefore, in determining the structure of the complex, the theoretical changes in the monomer units were imposed on the experimental structures of the free monomers to obtain values appropriate for the trimer. For the HF moieties, this amounts only to an adjustment of the values to which the HF bond lengths

(41) Marshall, M. D.; Muenter, J. S. *J. Mol. Spectrosc.* **1981**, *85*, 322.
(42) (a) Muenter, J. S.; Klemperer, W. *J. Chem. Phys.* **1970**, *52*, 6033. (b) Muenter, J. S. *J. Chem. Phys.* **1972**, *56*, 5409.
(43) Note that D_{HF} values used here are defined to be a factor of -2 times S_{HF} and that values reported by Muenter and Klemperer are actually $S_{HF}/(2J+3)(2J-1)$ for $J = 1$ and so have been multiplied by an additional factor of 5.
(44) Legon, A. C.; Rego, C. A. *Chem. Phys. Lett.* **1989**, *154*, 468.
(45) Although only $B - 2D_J$ has been determined, the difference is negligible from the point of view of structure determination.

Table 4. Structural and Energetic Parameters for $H_3N-HF-HF$[a]

		ab initio value (MP2/aug-cc-pVTZ)	
parameter	experimental value	non-CP	CP
r(N−F1)	2.4509(74)	2.5124	2.5328
r(F1−F2)	2.651(11)	2.5547	2.5771
∠(N−F1−F2)	77.47(25)	76.06	77.190
r(N−H1)	1.488(12)[d]	1.5303	1.5555
r(F1−H2)	1.738(17)[d]	1.6476	1.6722
r(H1−F1)	0.993145[e]	0.9953	0.9894
r(H2−F2)	0.944875[e]	0.9429	0.9411
r(N−H3)	1.10634[e]	1.0153	1.0149
r(N−H4)[b]	1.01365[e]	1.0122	1.0122
∠(N−H1−F1)	163(12)[d]	167.99	168.55
∠(H1−F1−H2)	95(2)[d]	90.53	91.34
∠(F1−H2−F2)	164(19)[d]	160.17	160.09
∠(H1−N−H3)	124(16)[d]	102.63	103.33
∠(H1−N−H4)[b]	105(6)[d]	115.02	114.92
∠(N−F1−H1)	11.0(8)	7.28	7.00
∠(F1−F2−H2)	12.0(11)	12.64	12.77
θ[c]	−5.7(45)	13.102	12.241
V_3 [cm^{-1}]	117.5818(13)[f]	125	108
D_e [kcal/mol]		23.46	21.95

[a] See Figure 3b for parameter definitions and atom labeling. All distances are in angstroms, and all angles are in degrees. [b] By symmetry, r(N−H4) = r(N−H5) and ∠(H1−N−H4) = ∠(H1−N−H5). [c] θ is the angle that the normal from the plane of the ammonia hydrogens to the nitrogen makes with the line joining N and F1. [d] Derived from fit parameters. [e] Determined by imposing theoretical changes on experimental values of monomers; held fixed in fits. For NH_3, values correspond to the asymmetric NH_3 structure described in the text. [f] Value for the parent isotopic form.

were constrained. For the NH_3 unit, the situation is somewhat more complicated: The most significant change in the ammonia monomer upon complexation is a 0.003 Å lengthening of the equilibrium distance of the NH bond in the HN−HF−HF ring. This removes the C_{3v} symmetry of the monomer, but since the NH_3 is rotating in the complex and the spectroscopic constants are related to the vibrationally averaged structure, it may be more appropriate to distribute the calculated changes equally among the three NH bonds. Since this is unclear, three NH_3 geometries were considered within the complex: (1) NH_3 with its bond distances and angles in the free monomer, (2) NH_3 with the theoretical changes imposed on the bond distances and angles of the free monomer, and (3) NH_3 with the average of the theoretical changes imposed on the bond distances and angles of the free monomer, so that the C_{3v} symmetry of the unit is retained. For asymmetric NH_3, which does not have a C_3 axis, a pseudo-C_3 axis was defined as the normal from the plane of the three hydrogens of the NH_3.

Structural parameters for $H_3N-HF-HF$ were determined from least-squares fits to the linear combinations of the rotational constants reported in Table 2 as well as cos δ, defined in eq 8. The final, "preferred" structure of the complex was derived from a series of such fits employing each of the three ammonia structures described above. Moreover, while the ab initio calculations predict an equilibrium geometry with a planar HN−HF−HF ring, it is likely that the HF units undergo some degree of angular excursion, which may move the vibrationally averaged position of the hydrogens from the NFF plane. The effect of this motion, however, was tested for each of the above ammonia structures using reasonable vibrational amplitudes based on H_3N-HF and $(HF)_2$[46] and was found to have an insignificant effect on the fitted structural parameters. The final structure parameters of the complex are given in Table 4 and represent averages from all fits performed, with uncertainties large enough to encompass the full range of results obtained. Several parameters derived from the fitted values are also given. For all fits, residuals in $(B + C)/2$ and $[A - (B + C)/2]$ were generally less than 0.5% (about 10 MHz) with the largest residual being nearly 50 MHz for $[A - (B + C)/2]$ of $ND_3-HF-HF$. For values of $(B - C)/2$, the residuals were generally somewhat larger, ranging from 15 to 35 MHz (∼2−4%). Residuals in cos δ were all smaller than 0.03, which corresponds to a difference of less than 3° in the angle δ. Several attempts were made to improve the quality of the structure fit, but it seems likely that, with the presence of several "soft" degrees of freedom in this complex, residuals of this magnitude may be inevitable.

Computational Methods and Results

To further explore the properties of the dimer and trimer, ab initio calculations were performed for HF, NH_3, HF−HF, H_3N-HF, and $H_3N-HF-HF$ using the aug-cc-pVTZ basis set[47] and second-order Møller−Plesset perturbation theory (MP2).[48] Since basis set superposition error (BSSE) can be significant for weakly bound systems, calculations were performed both with and without the counterpoise (CP) correction.[49] We note, however, that Del Bene and Shavitt caution that the counterpoise correction does not necessarily yield better energies for hydrogen bonded systems, and in fact, in some cases, may yield results which are farther from the fully converged values.[15a] Thus, in this work, we report results from both corrected and uncorrected calculations, which should bracket the true values. In performing these calculations, we have used the relatively new capability of MOLPRO 2000.1[50] that makes CP-corrected geometry optimizations straightforward. At the MP2/aug-cc-pVTZ level, results for H_3N-HF show the CP-corrected geometry to be closer to experiment, with the B rotational constant for the CP geometry 50 MHz higher than that observed, compared with 136 MHz higher for the non-CP value of B. The calculated equilibrium structures are similar to those obtained in previous theoretical studies.[22a,c,e23b,c,24d] Results are presented in Table 5, where the atom labeling for the trimer corresponds to that in Figure 3b.

The non-CP-corrected binding energies, D_e^{non-CP}, are the difference between the energy of the complex and the sum of the energies of the isolated monomers each with the monomer basis (mon-bs), viz

$$-D_e^{non-CP} = E_{complex} - \sum E_{mon,opt}^{mon-bs} \qquad (11)$$

The CP-optimized binding energy, D_e^{CP}, is defined as the difference between the complex energy and the monomer energies in the full basis of the complex (full-bs) minus the difference between the optimized monomers (mon,opt) and the monomers at their geometries in the complex (mon,comp), both in the monomer basis.

$$-D_e^{CP} = E_{complex} - \sum E_{mon,comp}^{full-bs} - \sum (E_{mon,opt}^{mon-bs} - E_{mon,comp}^{mon-bs})$$

(46) (a) Howard, B. J.; Dyke, T. R.; Klemperer, W. *J. Chem. Phys.* **1984**, *81*, 5417. (b) Gutowsky, H. S.; Chuang, C.; Keen, J. D.; Klots, T. D.; Emilsson, T. *J. Chem. Phys.* **1985**, *83*, 2070.

(47) (a) Dunning, T. H., Jr. *J. Chem. Phys.* **1989**, *90*, 1007. (b) Kendall, R. A.; Dunning, T. H., Jr.; Harrison, R. J. *J. Chem. Phys.* **1992**, *96*, 6796. (c) Woon, D. E.; Dunning, T. H., Jr. *J. Chem. Phys.* **1993**, *98*, 1358.

(48) (a) Møller, C.; Plesset, M. S. *Phys. Rev.* **1934**, *46*, 618. (b) Krishnan, R.; Frisch, M. J.; Pople, J. A. *J. Chem. Phys.* **1980**, *72*, 4244.

(49) Boys, S. F.; Bernardi, F. *Mol. Phys.* **1970**, *19*, 553.

(50) MOLPRO is a package of ab intio programs written by Werner, H.-J.; Knowles, P. J., with contributions from Amos, R. D.; Bernardsson, A.; Berning, A.; Celani, P.; Cooper, D. L.; Deegan, M. J. O.; Dobbyn, A. J.; Eckert, F.; Hampel, C.; Hetzer, G.; Korona, T.; Lindh, R.; Lloyd, A. W.; McNicholas, S. J.; Manby, F. R.; Meyer, W.; Mura, M. E.; Nicklass, A.; Palmieri, P.; Pitzer, R.; Rauhut, G.; Schütz, M.; Schumann, U.; Stoll, H.; Stone, A. J.; Tarroni, R.; Thorsteinsson, T.

Table 5. Computational Results for NH_3 and HF Species at the MP2/aug-cc-pVTZ Level, with and without Counterpoise Corrections[a]

	NH_3–HF–HF		NH_3–HF		HF–HF			
	non-CP	CP	non-CP	CP	non-CP	CP	NH_3	HF
r(N−F1)	2.5124	2.5328	2.6365	2.6522				
r(F1−F2)	2.5547	2.5771			2.7462	2.7708		
∠(N−F1−F2)	76.063	77.190						
r(N−H1)	1.5303	1.5555	1.6793	1.6965				
r(F1−H2)	1.6476	1.6722			1.8271	1.8527		
r(H1−F1)	0.9953	0.9894	0.9571	0.9557	0.9250	0.9248		0.9218
r(H2−F2)	0.9429	0.9411			0.9280	0.9276		
r(N−H3)	1.0153	1.0149	1.0124	1.0124			1.0121	
r(N−H4)[b]	1.0122	1.0122	1.0124	1.0124			1.0121	
∠(N−H1−F1)	167.988	168.551	180.000	180.000				
∠(H1−F1−H2)	90.534	91.336			114.245	115.037		
∠(F1−H2−F2)	160.170	160.087			170.279	169.888		
∠(H1−N−H3)	102.633	103.329	111.547	111.613			112.053	
∠(H1−N−H4)[b]	115.017	114.920	111.547	111.613			112.053	
∠(N−F1−H1)	7.283	7.002						
∠(F1−F2−H2)	12.635	12.768			6.452	6.741		
θ[c]	13.102	12.241						
μ_a[d] [D]	4.126	4.157	4.634	4.610	2.980	2.976		
μ_b[d] [D]	2.143	2.088			1.472	1.463		
μ_{total}[d] [D]	4.649	4.651	4.634	4.610	3.324	3.316	1.519	1.810
V_3 [cm^{-1}]	125	108						
D_e [kcal/mol]	23.46	21.95	12.93	12.28	4.71	4.23		

[a] All distances are in angstroms, and angles, in degrees. [b] By symmetry, r(N−H4) = r(N−H5) and ∠(H1−N−H4) = ∠(H1−N−H5). [c] θ is the angle that the normal from the plane of the ammonia hydrogens to the nitrogen makes with the line joining N and F1. [d] Dipole moments calculated at the CP-corrected and -uncorrected geometries.

Results with the aug-cc-pVTZ basis set show that, with the non-CP-corrected geometry optimizations, the binding energies of HF−HF, H_3N−HF, and H_3N−HF−HF are 4.7, 12.9, and 23.5 kcal/mol, respectively, whereas, with the counterpoise-corrected geometry optimizations, the binding energies decrease to 4.2, 12.3, and 22.0 kcal/mol. Thus, BSSE contributes at most 0.6 kcal/mol for H_3N−HF and 1.5 kcal/mol for H_3N−HF−HF. The binding energies are in reasonable agreement with previously published results and are summarized in Table 5. Also included in the table are values of the dipole moments, calculated at both the counterpoise-corrected and -uncorrected geometries.

In addition to the optimized structure and energetics, low-frequency large-amplitude vibrations and internal rotation are important in H_3N−HF−HF. To determine the barrier to internal rotation of the NH_3 unit, the binding energy of the complex was calculated at the MP2/aug-cc-pVTZ level as a function of the internal rotation angle, α, which is defined as the angle that one hydrogen of the ammonia makes with the NFF plane. Calculations were performed both with and without allowing relaxation of the molecular frame. The barrier to internal rotation of the NH_3 group was calculated to be as high as 3.0 kcal/mol without relaxation but drops to just 0.308 kcal/mol (108 cm^{-1}) with relaxation. Binding energy and structural parameters for a range of values for α are given elsewhere.[37]

Harmonic vibrational frequencies have been calculated using a non-CP-corrected approach and show the lowest frequency vibration of 79 cm^{-1} to be a ring-opening motion that increases the NFF angle. CP-corrected geometry optimizations at various NFF angles prove this motion to be quite anharmonic. The results are illustrated in Figure 4a, which is a plot of the complex binding energy as a function of the NFF angle. As this angle is changed, other significant changes occur within the complex. Most notably, as shown in Figure 4b, as the NFF angle is changed from its optimum value, the distances between the monomer units increase. A complete listing of structure parameters as a function of the NFF angle is given elsewhere.[37] The high-frequency vibration most affected by complexation is the stretching of the HF hydrogen bonded to the NH_3, with the calculated frequency dropping from 4123 cm^{-1} in free HF to 3339 cm^{-1} in H_3N−HF, and 2652 cm^{-1} in H_3N−HF−HF. The 3339 cm^{-1} value for H_3N−HF is in reasonable agreement with that of Del Bene and Jordan (3296 cm^{-1} in the harmonic approximation), though a two-dimensional anharmonic model reduces this value to 2832 cm^{-1} in their work.[6d]

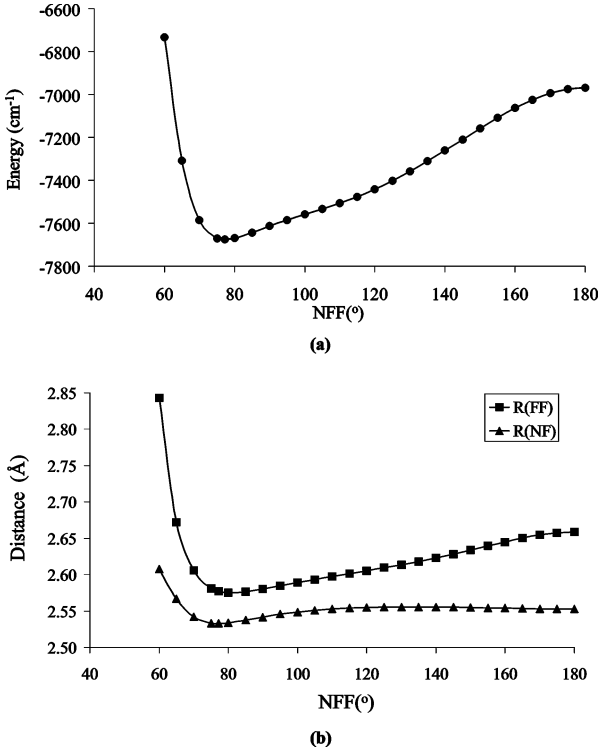

Figure 4. (a) Calculated binding energy for H_3N−HF−HF as a function of the N−F−F angle. (b) Calculated F−F and N−F distances as a function of the N−F−F angle.

Discussion

The experimental and theoretical results described above indicate, as expected, that the HF/NH_3 interaction in H_3N−HF is that of a classic hydrogen bond. Although the 1.69 Å N···H bond length is rather short in comparison with that in

NCCN−HF[51] or N_2−HF,[52] for example, in which the N···H distances are 1.94 and 2.16 Å, respectively,[53] it is considerably longer than the 1.0 Å covalent bond distance for an N−H bond.[54] The binding energy of 12−13 kcal/mol positions the interaction as a "moderate", almost "strong" hydrogen bond, according to the classification of Emsley,[1c,55] and the 19% reduction in the calculated harmonic HF stretching frequency is consistent with this assessment. The 0.03−0.04 Å elongation of the HF bond represents a distinct but modest increase in the degree of proton transfer. These results agree with numerous theoretical investigations, as well as the unpublished results reported over a decade ago.[20,26] The structural parameters given here constitute a refinement of the previously quoted values.

The structure of H_3N−HF−HF exhibits significant changes from the gas phase structures of the isolated H_3N−HF and $(HF)_2$ adducts. Most notably, comparison of the data reported in Tables 3 and 4 reveals that the addition of the extra HF unit to H_3N−HF decreases the N···H1 hydrogen bond length by 0.205(54) Å. Additionally, the N···F1 distance in the trimer is 0.19(3) Å smaller than that in H_3N−HF, and the F1···F2 distance is 0.14(2) Å shorter than the 2.79 Å value observed in $(HF)_2$.[46] The $(HF)_2$ portion of the trimer is also highly distorted, with an H1−F1···H2 angle nearly 30° smaller than that in the isolated dimer.[46] This smaller angle allows the outer fluorine to approach the in-plane hydrogen of the NH_3 unit and participate in another weak attractive interaction. Collectively, these changes reflect the two hydrogen bonds acting in concert to strengthen the overall interaction. Accordingly, the binding energy of the trimer exceeds the sum of the binding energies for H_3N−HF and $(HF)_2$ by 33%.[56]

The experimental changes in the distances between the NH_3 and HF units are similar to those predicted by the theoretical calculations. Figure 5 shows a comparison of the experimental and theoretical structures of the trimer, with an emphasis on the distances between the heavy atoms. Although the experimental values are related to the vibrationally averaged structure and the theory gives the equilibrium geometry, the agreement is remarkable. Distances and angles in the triangle formed by the heavy atoms differ by less than 0.082 Å and 2.3°, respectively. The excellent agreement between the theoretical and experimental structures provides strong evidence that the reported numbers should be quite reliable.

The 108 cm^{-1} internal rotation barrier of the NH_3 in the trimer, calculated with relaxation of the molecular frame, is also within 10% of the experimentally determined value, 118 cm^{-1}. The effect of allowing relaxation of the complex geometry along the internal rotation pathway is significant for this system. As the NH_3 rotates, the interaction with the outer fluorine is decreased and this loss is reflected in small increases in the distances between the monomer units and the N···F1···F2 angle. At the top of the barrier, r(N···F1) and r(F1···F2) have increased by 0.007 and 0.004 Å, respectively, and the N···F1···F2 angle is 5° larger than in the equilibrium structure. Similarly,

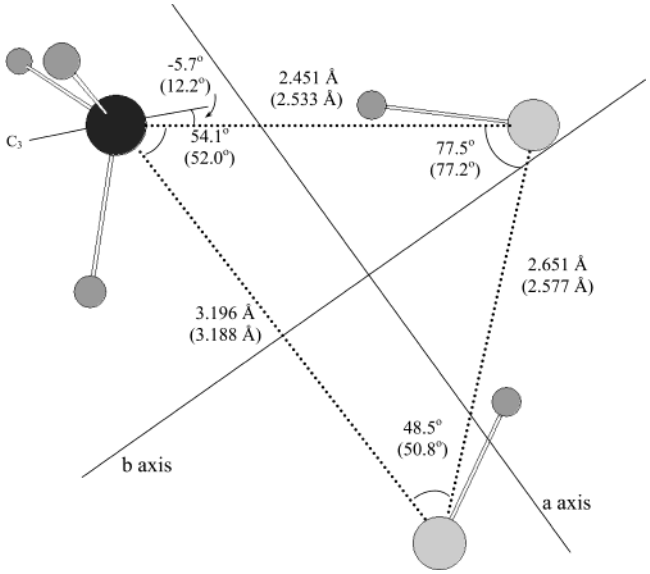

Figure 5. Structure of H_3N−HF−HF. Theoretical values are given in parentheses. Although the experimentally determined value of θ is negative, a positive value is shown here for the sake of clarity of the drawing. The *a*- and *b*-inertial axes are shown for the parent isotopic form.

changes in the structure occur as the molecule undergoes the low-frequency vibration associated with a change in the N···F1···F2 angle. This ring-opening motion also has the effect of diminishing the secondary interaction between the outer fluorine and the in-plane NH_3 hydrogen.

The ab initio value of the dipole moment of the trimer (at the CP-corrected structure) is 4.651 D, with components 4.157 and 2.088 D along the *a*- and *b*-inertial axes of the complex, respectively. Interestingly, the individual dipole moment projections for the H_3N−HF and HF units add along the *a*-axis and oppose along the *b*-axis, with the result that the net dipole moment of the trimer, after polarization, is almost identical to that of H_3N−HF (4.610 D at the CP-corrected geometry). If the complex is considered to consist of separate H_3N−HF and HF units with dipole moments within the trimer of μ_1 and μ_2, respectively, we can use the calculated values of μ_a and μ_b to estimate the values of μ_1 and μ_2, since the location of the inertial axes within the complex is known. Using Cartesian coordinates for the CP-corrected, optimized structure and values of μ_a and μ_b calculated for that structure, we estimate that $\mu_1 = 5.15$ D and $\mu_2 = 2.39$ D, which may be compared with the ab initio values for "free" H_3N−HF and HF of 4.61 and 1.81 D, respectively. Thus, we conclude that complexation induces approximately half a Debye moment in each of the moieties.

According to the calculations, the addition of the second HF molecule decreases the stretching frequency of the inner HF by 687 cm^{-1}, indicating a significant weakening of this bond and a greater degree of proton transfer. The infrared spectra in an argon matrix show an even larger shift of this stretching frequency, which is 3041 and 1920 cm^{-1} for the 1:1 and 1:2 H_3N/HF complexes, respectively.[18c] The lower frequency of this stretch in the trimer lies in the region for shared proton vibrations, and the adduct is considered to be a hydrogen bonded complex involving a bifluoride anion, viz, $H_3N{-}H^+{-}(F{-}H{-}F)^-$. In the gas phase structure of H_3N−HF−HF, the proton of the primary hydrogen bond is approximately 0.5 Å closer to the fluorine than the nitrogen and, therefore, would not be considered a fully shared proton.

(51) Legon, A. C.; Soper, P. D.; Flygare, W. H. *J. Chem. Phys.* **1981**, *74*, 4936.
(52) Soper, P. D.; Legon, A. C.; Read, W. G.; Flygare, W. H. *J. Chem. Phys.* **1982**, *76*, 292.
(53) These values of the hydrogen bond lengths are derived from the reported N···F distances and the free HF bond length of 0.926 Å.
(54) Cotton, F. A.; Wilkinson, G. *Advanced Inorganic Chemistry*, 3rd ed.; Wiley-Interscience: New York, 1972.
(55) Emsley, J. *Chem. Soc. Rev.* **1980**, *9*, 91.
(56) The 33% value applies for both the CP-corrected and -uncorrected binding energies.

However, it is reasonable that the argon matrix increases the degree of proton transfer, as matrix effects are certainly well-known in the spectra of amine−HX [18,19] and amine−$(HF)_2$ [18h] complexes.

It is of interest to attempt to further quantify what the experimental and theoretical results reported above mean in terms of the ability of the additional HF molecule to promote proton transfer in the gas phase. Surely, no single measure of proton transfer is uniquely ideal, and indeed a variety of physical properties, including quadrupole coupling constants,[20] vibrational frequencies,[2,6b,17b] and bond distances,[2,57] have been used to gauge the relative contribution of hydrogen bonded and proton-transferred forms. Since the work reported here is primarily structural, a particularly convenient parameter is that defined by Kurnig and Scheiner,[57] who have focused on HX and N···H bond distances, defining a "proton-transfer parameter"[58]

$$\rho_{PT} = (r_{HX} - r^{\circ}_{HX}) - (r_{NH} - r^{\circ}_{NH}) \qquad (13)$$

where r°_{HX} and r°_{NH} are the HX and NH bond lengths in free HX and covalently bonded R_3NH^+, respectively, and r_{HX} and r_{NH} are those in the complex of interest. Thus, ρ_{PT} assesses proton transfer according to how much the HX bond stretches in the complex *and* how much the N···H distance exceeds that in a system with full proton transfer. In a purely hydrogen bonded complex, the first term vanishes and $\rho_{PT} < 0$, while, for a true ion pair, the second term vanishes and $\rho_{PT} > 0$. When the stretching of the HX bond is equal to the elongation of the N···H distance relative to the covalent bond distance, $\rho_{PT} = 0$, and the proton is considered equally shared between the donor and acceptor. Using ab initio methods, Kurnig and Scheiner obtained a value of $\rho_{PT} = -0.65$ for H_3N-HF, which lies at or near the purely hydrogen bonded limit. For $(CH_3)_3N-HBr$, on the other hand, a value of $\rho_{PT} = -0.05$ was obtained, indicating a nearly equal sharing of the proton between the amine and the halogen.

Using the results of this study, values for ρ_{PT} can be calculated for both H_3N-HF and $H_3N-HF-HF$. For H_3N-HF, the ab initio value of 0.034 Å for the elongation of the HF bond, together with the experimental N···H distance in the dimer and an N−H covalent bond length of 1.0 Å,[54] gives a value of $\rho_{PT} = -0.66$ Å. This value is in excellent agreement with the much older, theoretical value of −0.65. For $H_3N-HF-HF$, our computed elongation of the HF bond is 0.068 Å, and using the experimental N···H distance (1.488 Å), the calculated value of ρ_{PT} increases to −0.42. It is worth noting that while these results rely on computed values for the HX distances, the contribution from the first term in eq 13 is small. Indeed, the value of ρ_{PT}, as well as its change upon addition of an extra HF moiety, is dominated by the shrinkage of the N···H hydrogen bond.

The value of $\rho_{PT} = -0.42$ Å obtained for $H_3N-HF-HF$ is comparable to that previously calculated by Krunig and Scheiner for the complex $(CH_3)H_2N\cdots HCl$.[57] This value, however, represents the results of uncorrelated calculations with a minimal basis set and is, therefore, likely to be quantitatively inaccurate. Thus, to gain a better picture as to what the experimental value of ρ_{PT} means, we used the results of several more modern computational studies[22a,b,24c,d] to estimate ρ_{PT} for a series of amine−hydrogen halide complexes. For H_3N-HCl, values of ρ_{PT} range from −0.65 to −0.75 (depending on the basis set used and method of calculation) and, as such, represent a degree of proton transfer similar to that in the H_3N-HF dimer. Values for $(CH_3)_3N-HCl$, on the other hand, are in the vicinity of +0.15 to +0.25, which is considerably larger than that for either H_3N-HF or $H_3N-HF-HF$. We also used the experimental results for $(CH_3)_3N-HF$[44] to determine a value of $\rho_{PT} = -0.57$ for that complex. These numbers show that, to the extent that the degree of proton transfer is properly measured by ρ_{PT}, proton transfer in $H_3N-HF-HF$ is greater than that in either H_3N-HCl or $(CH_3)_3N-HF$ but less than that in $(CH_3)_3N-HCl$. Clearly, a single, additional HF molecule has a significant effect on the complex, larger than that arising from a methylation of the ammonia or from substitution of the fluorine by chlorine. However, the effect is not enough to bring the system fully into the proton shared regime. Interestingly, computational results by Heidrich[22c] affirm the hydrogen bonded nature of $H_3N-(HF)_2$ and predict the most stable form of $H_3N-(HF)_3$ to also be a hydrogen bonded molecular complex. However, the addition of the third HF gives rise to a second, less stable potential energy minimum corresponding to a contact ion pair.[59] Thus, it is perhaps not too surprising to find that the complex with only two HF molecules shows what one might term "early signs" of proton transfer.

Finally, it is interesting to note that recent calculations by two groups[23b,c] on $H_3N-HF-(H_2O)_n$ indicate a 0.094 Å reduction in the N···H bond distance and a 0.020 Å increase in the HF bond length upon addition of a single water molecule. While comparable in magnitude to those observed here, these numbers are clearly smaller than the corresponding values for $H_3N-HF-HF$ (0.21 Å and 0.068 Å, respectively). Whether this difference is real or whether the calculations underestimate the size of these changes is not clear. In either case, presumably, the strongly polar "microsolvent" stabilizes a small amount of charge separation associated with partial proton transfer, but a quantitative comparison based on dipole moments and complex geometry does not appear straightforward.

Summary

The complexes H_3N-HF and $H_3N-HF-HF$ have been examined by microwave and ab initio techniques. The H_3N-HF complex is a fairly strongly hydrogen bonded system, in agreement with much previous experimental and theoretical evidence. $H_3N-HF-HF$ is also a hydrogen bonded complex, but the addition of the second HF molecule promotes measurable change in the degree of proton sharing. Most striking is a 0.21(6) Å contraction of the primary N···H hydrogen bond relative to that in H_3N-HF, a complex whose hydrogen bond is already rather short. For the HF moiety hydrogen bonded to the NH_3, ab initio calculations indicate a 0.068 Å elongation of the HF bond relative to that in free HF. These changes have been used to assess the degree of proton transfer according to a hydrogen bonding parameter previously defined,[57] and the results suggest

(57) Kurnig, I. J.; Scheiner, S. *Int. J. Quantum Chem., Quantum Biol. Symp.* **1987**, *14*, 47.

(58) We use the subscript "PT" to distinguish the proton-transfer parameter from the magnitude of the vector defined in eq 6. Thus, ρ_{PT} in this work is equivalent to the ρ of Kurnig and Scheiner.

(59) Note that the structure of the contact ion pair in this case does not correspond to that obtained simply by proton transfer across the primary N···H hydrogen bond. Considerable rearrangement of the HF molecules also accompanies the transformation from the molecular complex to the proton transferred form.

that the presence of a single additional HF molecule to H_3N-HF increases the proton transfer to a degree greater than that in H_3N-HCl and $(CH_3)_3N-HF$ but less than that in $(CH_3)_3N-HCl$. It is well-known that the creation of a crystalline environment stabilizes the charge separation associated with proton transfer, but it is less clear, in general, how many individual, polar near-neighbors are sufficient to render such transfer complete. This study shows that a single, polar near-neighbor, while insufficient to fully stabilize the ionic form, can have a significant effect. This conclusion is similar to that which we have recently drawn for the electron pair transfer complexes $HCN\cdots HCN-SO_3$[60] and $HCN\cdots HCN-BF_3$,[61] in which the addition of the outer HCN produces significant advancement in the degree of dative bond formation. These studies demonstrate that acid−base complexes, both of the Brønsted and the Lewis types, constitute a particularly interesting class of systems in which to study microsolvation effects, as large changes can be observed, even at the rather small cluster level.

Acknowledgment. This work was supported by the National Science Foundation, the donors of the Petroleum Research Fund, administered by the American Chemical Society, and by the Minnesota Supercomputer Institute. Funding from a Camille and Henry Dreyfus Postdoctoral Fellowship in Environmental Science (K.J.H.) is also gratefully acknowledged.

Supporting Information Available: Tables of transition frequencies and assignments for H_3N-HF and $H_3N-HF-HF$ and their isotopic derivatives. This material is available free of charge via the Internet at http://pubs.acs.org.

JA030435X

(60) Fiacco, D. L.; Hunt, S. W.; Leopold, K. R. *J. Phys. Chem. A* **2000**, *104*, 8323.
(61) Fiacco, D. L.; Leopold, K. R. *J. Phys. Chem. A* **2003**, *107*, 2808.